

Focusing of Light by a Nano-Hole Array

Fu Min Huang¹, Yifang Chen², F. Javier Garcia de Abajo³ and Nikolay Zheludev¹

¹*Optoelectronics Research Center, University of Southampton, SO17 1BJ, UK,*

²*Central Microstructure Facility, Rutherford Appleton Laboratory, Didcot, OX11 0QX, UK,*

³*Instituto de Optica, CSIC, Serrano 121, 28006 Madrid, Spain*

(Dated: November 9, 2006)

We demonstrate a conceptually new mechanism for focusing at optical frequencies based upon the use of nano-hole quasi-periodic arrays in metal screens. Using coherent illumination at 660nm and scanning near-field optical microscopy, $\sim 290\text{nm}$ "hot spots", were observed at a distance of $\sim 12.5\mu\text{m}$ from the array. Even smaller hot-spots of about 200nm in waist were observed closer to the plane of the array.

Nano-holes and arrays of nano-holes in metal screens show a number of intriguing optical properties, most notably the extraordinarily high transmission of regular [1] and quasi-periodic [2] hole arrays and unusual polarization-sensitive effects [3, 4]. Here we show for the first time that a quasi-crystal array of nano-holes in a metal screen can "focus" light at distances up to several tens of wavelengths from the screen. It produces bright foci of energy concentration, harvesting energy from a large number of holes in the array. The foci are sparsely distributed in the "focal plane".

The "focusing" of light was observed with a quasi-crystal array illuminated with a coherent light source. The array had approximate 10-fold symmetry and contained about 14,000 holes of 200nm diameter. The overall diameter of the array was $\sim 0.2\text{mm}$. The array comprised a Penrose-like pattern manufactured in accordance with the algorithm described in reference [5]. It was manufactured by electron beam lithography in a 100nm aluminium film deposited on a silica substrate (see Fig. 1i). The high level of positional accuracy achieved in the manufacturing of the holes may be judged from a comparison of the far-field diffraction pattern produced by the array and the reciprocal lattice, calculated from the prescribed coordinates of the holes. Allowing for expected axial distortion and scaling these should be congruent mappings of each other, and indeed they are (compare Fig. 1(ii) and Fig. 1(iii)).

To map the field distributions created by the array we used a scanning near-field optical microscope (Omicron TwinSNOM R/T) operating in transmission mode, with light collected through a metal-coated tapered fiber tip with an aperture of about 120nm (Fig.1-iv). As optical sources we used either diode lasers operating at 660nm and 635nm or a continuum fiber laser and a selection of 40nm bandpass filters. Fig. 2 shows characteristic field maps measured at different heights h above the plane of the array for two different wavelengths, thus illustrating the variety of "photonic carpet" patterns generated by the quasi-crystal structure. In most cases, the carpets show elements of approximate 5-fold or 10-fold symmetry. In the immediate proximity of the sample (scans (i) and (ii)), the optical field concentrates at the holes. Further

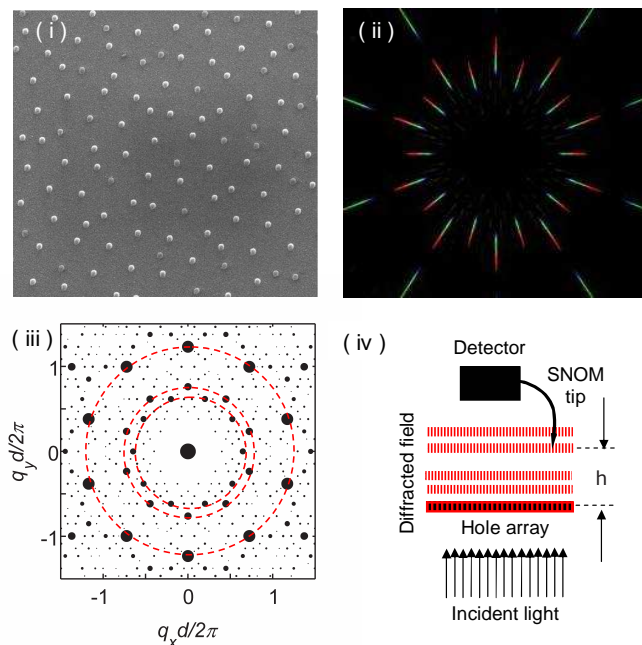


FIG. 1: The quasi-crystal sample and its reciprocal lattice. (i) An SEM image of a fragment ($20 \times 20\mu\text{m}$) of the quasi-crystal array of holes; (ii) far-field diffraction pattern of the quasi-crystal array, obtained with white light illumination; (iii) the reciprocal lattice of the quasi-crystal array wherein spot diameter is proportional to the magnitude of the spectral component. The minimum distance between two neighbouring holes $d = 1.2\mu\text{m}$. Red dashed circles show several "partial" Montgomery rings; (iv) schematic of the experiment showing diffraction field pattern over the array illuminated with coherent light.

away from the array, the pattern changes dramatically and blurry, defocused patterns (v), (vi), alternate with well-defined arrangements of hot-spots (iii), (iv), (vii), (viii) that appear at specific, irregular heights. At some heights and wavelengths bright foci, separated by a few microns from the neighbouring spots, are seen (scans (vii) and (viii)). The patterns depend not only on the wavelength and height, but also on the distance between the focus of the illuminating lens and the quasi-crystal structure.

Fig. 3 shows a detailed scan of the foci at two charac-

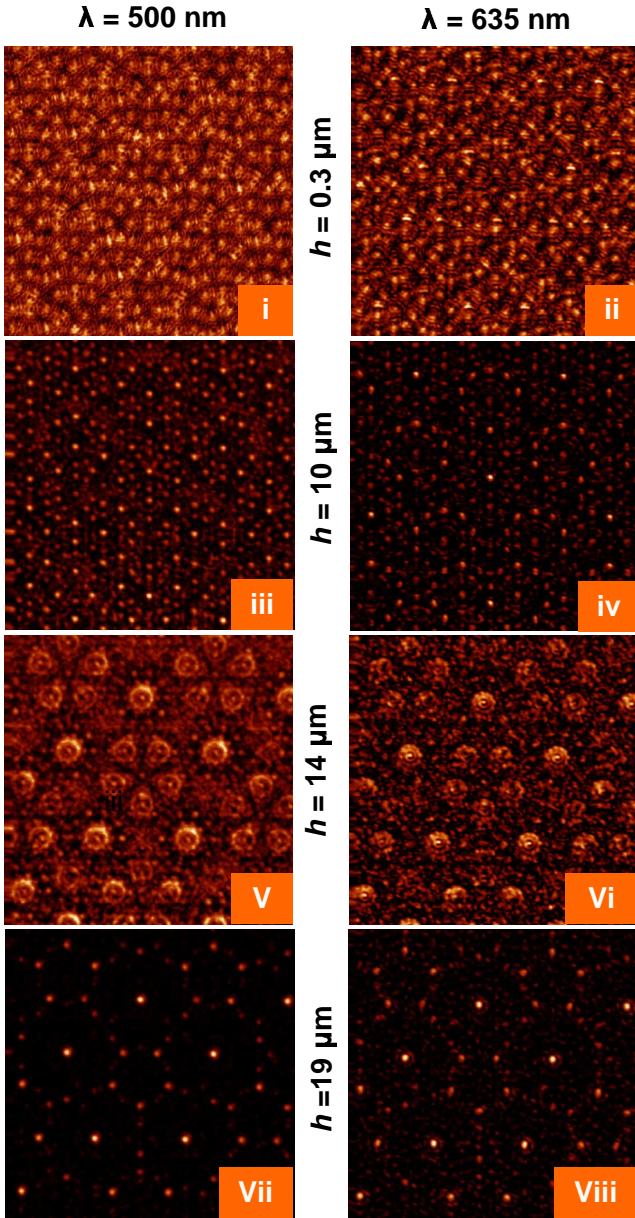


FIG. 2: Field maps at different heights h above the quasi-crystal array of holes. Each scan is $30\mu\text{m} \times 30\mu\text{m}$ in area. The images were obtained by SNOM using illumination wavelengths of 500nm (upper row) and 635nm (lower row). Note the highly isolated hot-spots observed at $h = 66\mu\text{m}$ for the 500nm excitation wavelength and at $h = 14\mu\text{m}$ for the 635nm excitation wavelength.

teristic distances, with the array illuminated at a wavelength of 660 nm . At a distance of about $5\mu\text{m}$ from the array, a relatively dense pattern of hot-spots is seen. Here the bright foci are elliptical with a FWHM of 375nm along the polarization direction of the incident light and 235nm in the perpendicular direction. After deconvolution to account for the aperture size of the SNOM probe, the actual size of the hot-spots is estimated to be about $360 \times 200\text{nm}$ ($0.54\lambda \times 0.30\lambda$). A much clearer pattern

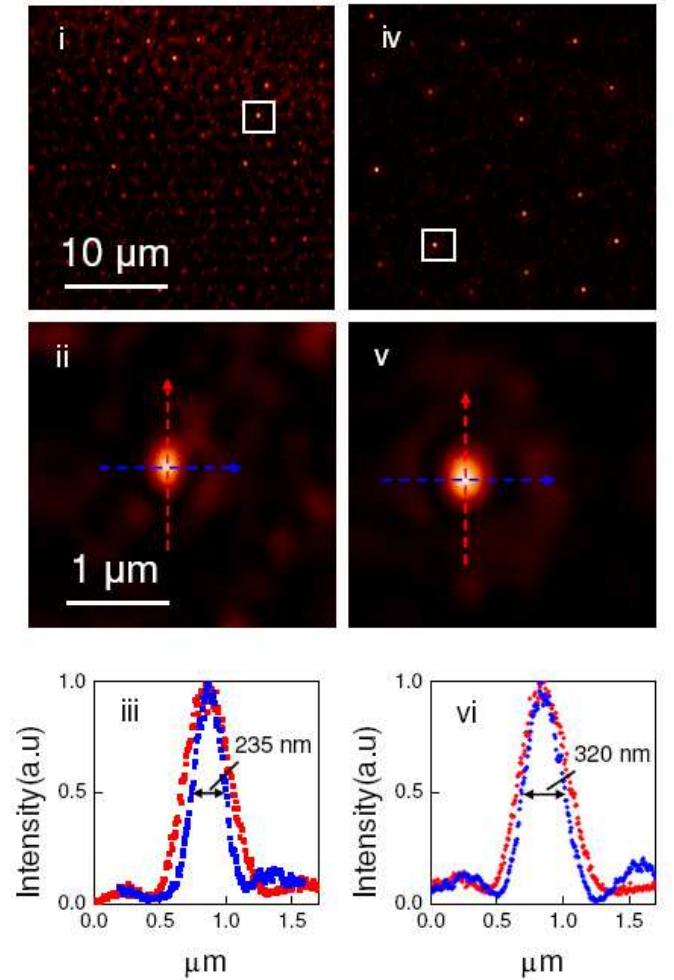


FIG. 3: Subwavelength hot-spots formed at different heights above the quasi-crystal array. The illumination source is a diode laser with a wavelength of 660nm . (i) field map at a height $h = 5\mu\text{m}$ above the array; (ii), (iii) fine scan image of the hot-spot indicated in map (i) and corresponding profiles of the focus along directions parallel (blue dots) and perpendicular (red dots) to the polarization of the incident light; (iv) field map at a height $h = 12.5\mu\text{m}$ above the array; (v), (vi) fine scan image of the hot-spot indicated in map (iv) and corresponding profiles of the focus along directions parallel (blue dots) and perpendicular (red dots) to the polarization of the incident light.

of well-isolated hot-spots is seen at a distance of about $12.5\mu\text{m}$ from the array. Here the scanned cross-sectional dimensions are $420 \times 320\text{nm}$, and after deconvolution the spot size obtained is about $400 \times 290\text{nm}$ ($0.60\lambda \times 0.44\lambda$). Thus, the structure produces bright foci of energy concentration by harvesting energy from a large number of holes. For example, in Fig. 2-vii the density of the brightest hot-spots (arranged in pentagons), which receive the majority of the energy, is some 40 times lower than that of the holes in the array.

This new phenomenon of "lensing" by the nano-hole array results from the partial reconstruction of the ar-

ray's field in the diffraction zone, in a manner analogous to the classical Talbot effect [6] observed with periodic gratings, where diffraction leads to the reconstruction of the grating's field at periodic distances from the grating. In the Talbot effect a grating with period a images itself at multiples of the Talbot distance $h_T = a^2/\lambda$ when illuminated with a coherent plane wave. In the paraxial approximation, an infinitely long grating will be perfectly reconstructed at the Talbot distance. Montgomery [7] has shown that a wide range of patterns can image themselves, with linear periodic grating being only one example. A pattern will show full reconstruction at a distance h if its spatial frequencies are discrete and located in the reciprocal plane at rings of radii $m^2 = 1/\lambda^2 - (m/h)^2$, where m is an integer such that $0 \leq m \leq h/\lambda$. For instance, circular or linear diffraction gratings are self-imaging objects whose spectra in the reciprocal lattice are sets of equidistant rings or dots, respectively. The spectrum of the quasi-periodic array lies somewhere between the dotted spectrum of a linear grating and the rings of a circular grating. However, as the rich spectrum of frequencies of the quasi-periodic array are located on circles (as shown in Fig. 1ii) the Montgomery condition is fulfilled for all spectral maxima, but not necessarily simultaneously. Therefore the self-imaging distance h will be different for different rings of maxima on the reciprocal lattice, and for different wavelengths. Moreover, when a regular grating is illuminated with a divergent beam, the reconstructed image is magnified, so the reconstructed field does not necessarily have the same period as the original grating. Similarly, when partial reconstruction of the quasi-periodic array takes place, the pattern of reconstructed hot-spots has the appearance of a scaled partial image of the array. Thus, reconstruction of a quasi-periodic array of holes is a complex process which may be envisaged as a superposition of a large number of partial reconstructions happening at different heights at the array. With varying height h , one will see a continuous evolution of partially reconstructed images of the array. What is important however, is that at some distances and wavelengths well defined sparsely distributed foci are seen. To illustrate this process of quasi-periodic grating reconstruction, we have calculated the field intensity maps created by quasi-crystal array using the scalar diffraction theory. The calculation gives very good agreement with experiential results as is illustrated by Fig.4.

In conclusion, the focusing of coherent light by a quasi-crystal array of holes has been observed at distances ranging from a few microns to a few tens of microns from the plane of the array. With focused hot-spots of such high localization and brightness, resolution exceeding that of

sophisticated high-numerical aperture lenses imaging can be achieved by scanning the object under investigation across the focal spot. Similarly, a single hot-spot appropriately isolated by a mask may be used as a "light pen" in high resolution photo-lithography.

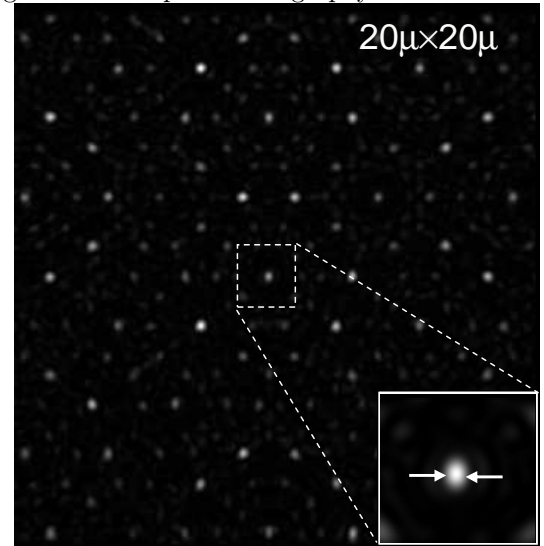


FIG. 4: Theoretical calculations at the conditions close to that of Fig 2-iii show a pattern similar to that observed experimentally and give hot-spots of 220nm in cross-section.

Acknowledgements. Acknowledgements. This work was supported by the EPSRC. We thank Nikitas Paspasimakis and Alexander Schwanecke for taking far-field diffraction patterns of the array and Kevin Macdonald for help in preparing the manuscript.

-
- [1] T.W. Ebbesen, H.J.Lezec, H.F.Ghaemi, T.Thio, P.A. Wolff, *Nature* **391**, 667 (1998).
 - [2] A.S. Schwanecke, N. Paspasimakis, V.A.Fedotov, F.M. Huang, Y. Chen, F.J. Garca de Abajo, N.I. Zheludev, *Nanophotonics Topical Meeting*, Uncasville, CT, USA, 24 - 28 Apr 2006; F. Przybilla, C. Genet, and T. W. Ebbesen. *Appl. Phys. Lett.* **89**, 121115 (2006).
 - [3] A.V.Krasavin, A.S.Schwanecke, M. Reichelt, T. Stroucken, S. Koch, E.M. Wright, N.I. Zheludev, *Appl. Phys. Lett.* **86**, 201105 (2004).
 - [4] J. Elliott, I.I. Smolyaninov, N.I. Zheludev, A.V. Zayats, *Phys. Rev. B* **70**, 233403 (2004).
 - [5] E.A.Lord, K. Ramakrishnan, S. Ranganathan, *Bull. Mater. Sci.* **23**, 119 (2000).
 - [6] K. Patorski, *Progress in Optics* **27**, 3 (1989).
 - [7] W.D.Montgomery, *J. Opt. Soc. Am.* **57**, 772 (1967).